Neuron, Vol. 45, 433–445, February 3, 2005, Copyright ©2005 by Elsevier Inc. DOI 10.1016/j.neuron.2004.12.049

GABA Transporter Currents Activated by Protein Kinase A Excite Midbrain Neurons during Opioid Withdrawal

Elena E. Bagley,* Michelle B. Gerke, Christopher W. Vaughan, Stephen P. Hack, and MacDonald J. Christie
Pain Management Research Institute
at Royal North Shore Hospital
The University of Sydney
NSW 2006
Australia

Summary

Adaptations in neurons of the midbrain periaqueductal gray (PAG) induced by chronic morphine treatment mediate expression of many signs of opioid withdrawal. The abnormally elevated action potential rate of opioid-sensitive PAG neurons is a likely cellular mechanism for withdrawal expression. We report here that opioid withdrawal in vitro induced an opioid-sensitive cation current that was mediated by the GABA transporter-1 (GAT-1) and required activation of protein kinase A (PKA) for its expression. Inhibition of GAT-1 or PKA also prevented withdrawal-induced hyperexcitation of PAG neurons. Our findings indicate that GAT-1 currents can directly increase the action potential rates of neurons and that GAT-1 may be a target for therapy to alleviate opioid-withdrawal symptoms.

Introduction

Opioids are intensely addictive, and cessation of their chronic use is associated with a withdrawal syndrome consisting of severe early physical symptoms and late features such as craving. Relapse into drug-taking behaviors often occurs as a result of this withdrawal syndrome (Mattick and Hall, 1996; Williams et al., 2001), which is thought to result from neuronal adaptations that develop to restore homeostasis during chronic opioid exposure (Himmelsbach, 1943). On cessation of opioid administration, persistent counteradaptations in critical brain regions are unmasked and cause the withdrawal syndrome. A rebound increase of adenylyl cyclase/protein kinase A (PKA) signaling is one counteradaptation that has been implicated in the expression of opioid-withdrawal signs (Sharma et al., 1975; Nestler and Tallman, 1988; Terwilliger et al., 1991).

The midbrain periaqueductal gray (PAG) is crucial for expression of many somatic signs of opioid withdrawal. Studies using microinjections of opioid antagonists and agonists indicate that the PAG is involved in the expression of physical withdrawal signs such as teeth chattering, wet-dog shakes, and eye twitch, as well as escape behaviors and place aversion (Bozarth and Wise, 1984; Stinus et al., 1990; Maldonado et al., 1995; Punch et al., 1997). While opioid agonists acutely inhibit adenylyl cyclase activity in the brain (Collier and Roy, 1974) and specifically in the PAG (Fedynyshyn and Lee, 1989), there is a compensatory increase in adenylyl cyclase signaling during chronic treatment with morphine in vitro (Sharma et al., 1975; Avidor-Reiss et al., 1997) and in vivo (Terwilliger et al., 1991) resulting in rebound hyperactivity of this cascade during withdrawal. Microinjections of PKA inhibitors into the PAG attenuate a spectrum of opioid-withdrawal behaviors similar to those induced by microinjections of opioid antagonists (Maldonado et al., 1995; Punch et al., 1997). One cellular mechanism by which elevated adenylyl cyclase signaling could produce behavioral signs of withdrawal is the hyperexcitation of opioid-sensitive PAG neurons (Chieng and Christie, 1996). Increased adenylyl cyclase signaling has also been proposed to result in the increased action potential rates of neurons in other brain regions during opioid withdrawal (Kogan et al., 1992; Nestler et al., 1999; Ivanov and Aston-Jones, 2001).

We aimed to determine adaptations in PAG neurons that result in hyperexcitation of action potential rate during withdrawal and whether PKA is involved in this process. Whole-cell, cell-attached, and perforated patch recordings of PAG neurons from mice chronically treated with morphine were used to demonstrate that opioid withdrawal increases a GABA transporter-1 (GAT-1) cation current. The increased GAT-1 current is dependent on PKA activity and is associated with the withdrawal-induced elevated action potential rate of PAG neurons. Thus, we have established that opioid withdrawal stimulates a GAT-1 current that increases the excitability of PAG neurons and is dependent on PKA activation.

Results

Opioid Withdrawal Elevates the Action Potential Rate

We first tested whether opioid withdrawal affected the action potential rate of mouse PAG neurons as it does in the rat (Chieng and Christie, 1996). Slices from vehicle- and morphine-treated mice were incubated in morphine (5 μM), and the opioid antagonist naloxone (1 μM) was added to cause withdrawal. The AMPA/kainate receptor antagonist CNQX (10 μM) and the $GABA_A/GABA_C$ antagonist picrotoxin (100 μM) were present during these experiments. In slices from vehicle-treated control mice, naloxone superfusion produced a small increase in action potential rate as measured using cell-attached recordings (Figures 1A and 1C; increase from 2.7 ± 1.5 Hz to 3.8 ± 1.1 Hz, only physiologically healthy neurons were analyzed, see Experimental Procedures). In morphine-treated mice, naloxone produced a significantly larger increase in action potential rate (Figures 1B and 1C; increase from 2.6 ± 0.36 Hz to 6.7 ± 1.05). Thus, as in rat, opioid withdrawal hyperexcited mouse PAG neurons.

Naloxone did not increase the action potential rate of all neurons. However, not all PAG neurons are opioid sensitive (Chieng and Christie, 1994; Osborne et al., 1996; Vaughan et al., 2003), and withdrawal-induced

*Correspondence: bagleye@med.usyd.edu.au

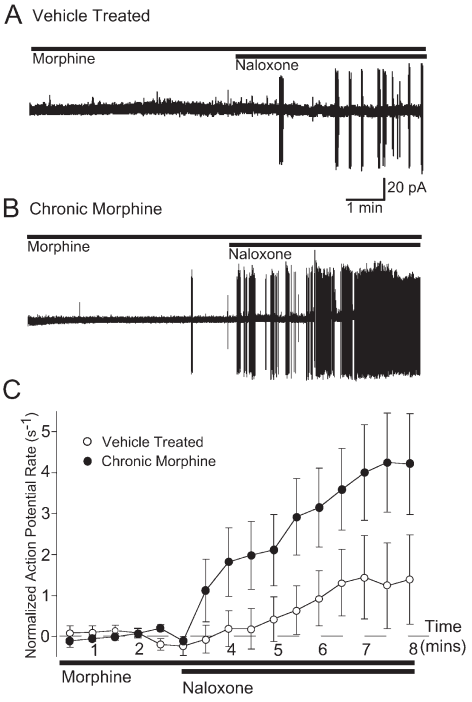

Figure 1. Opioid Withdrawal Elevates the Action Potential Rate in PAG Neurons

(A and B) Spontaneous action potential currents were measured during cell-attached recordings (drug superfusion shown by bars). (A) Naloxone (1 μM) increased the action potential rate of a control neuron maintained in morphine (5 μM). (B) Naloxone (1 μM) substantially increased the action potential rate of a neuron from a morphine-treated mouse maintained in morphine (5 μM).

(C) Normalized rate histograms (data point every 30 s) were generated. Action potential rate for each neuron was normalized to the first seven points (n = 33 for control, n = 40 for chronic morphine). The naloxone-induced increase in the action potential rate of neurons from morphine-treated mice (filled circle) was significantly greater than control (open circle, 8 min time point, $p < 0.05$.)

hyperexcitation occurs in opioid-sensitive but not -insensitive PAG neurons (Chieng and Christie, 1996). Because postsynaptic opioid sensitivity could not be determined during the cell-attached recordings in the present study, the average increase in excitability (Figure 1C) represents an underestimate of the withdrawal excitation of opioid-sensitive neurons.

Chronic Morphine Treatment Induces an Additional Opioid-Sensitive Conductance

G protein-gated inward rectifier potassium (GIRK) channels underlie the inhibition by morphine of PAG action potential rates in neurons from untreated animals (Chieng and Christie, 1994; Vaughan et al., 2003). However, in morphine-treated rats, in vitro, withdrawal by naloxone was not explained by reversal of opioid activation of GIRK channels, because the current did not reverse polarity at E_K (Chieng and Christie, 1996). This suggests that withdrawal from chronic opioid treatment modulates an additional opioid-sensitive current. To allow activation and therefore study of the withdrawal-induced current, slices from morphine- and vehicle-treated mice were spontaneously withdrawn (morphine-free ACSF for >1 hr). In slices from vehicle-treated mice, the opioid agonist methionine-enkephalin (MENK, 30 μM) produced an outward current in PAG neurons (Figure 2A, 39 of 42 neurons voltage clamped at −56 mV) that resulted from potassium channel activation because the reversal potential of the current was close to the potassium reversal potential (Figures 2C and 2E; −110 mV ± 3 mV, n = 39; E_k calculated with the Nernst equation was −103 mV; nonreversing currents were assigned a nominal reversal potential of −136 mV, the most negative potential that could be achieved without disrupting recordings). By contrast, the MENK-induced outward current during spontaneous withdrawal (Figure 2B) did not reverse polarity close to E_k, indicating that opioids no longer solely activated a K conductance (Figures 2D and 2E; n = 37). The MENK-induced currents from both morphine- and vehicle-treated mice were unaffected by blockers of synaptic transmission (CNQX [5–10 μM], picrotoxin [100 μM], or bicuculline methiodide [30 μM] and tetrodotoxin [TTX] [0.3–1 μM]), so the results with and without blockers were combined (Figure 2E). These synaptic transmission blockers were present in all subsequent experiments, and TTX was included in all experiments not examining action potentials. The MENK-induced currents in slices from morphine-treated mice resulted from μ-opioid receptor activation, as they were fully blocked by the μ-opioid receptor-selective antagonist CTAP (1 μM; MENK current was 1 ± 2 pA at −56 mV in CTAP, n = 4). The μ-opioid receptor-selective agonist DAMGO (1 μM) also induced a nonreversing outward current (16 ± 3 pA at −56 mV, n = 3).

The lack of a measurable reversal potential for the MENK current during morphine withdrawal is consistent with MENK simultaneously increasing and/or decreasing the activity of two conductances. These results therefore suggest that, after chronic opioid treatment, withdrawal activates an additional opioid-sensitive current that can be inhibited by readdition of opioid agonists. An additional, non-GIRK opioid-conductance might also be occasionally modulated in neurons from vehicle-treated mice (nonreversing MENK current in 4 of 39 cells). However, it is modulated in the majority of neurons during opioid withdrawal (nonreversing MENK current in 24 of 37 cells, $\chi^2 = 24.36$, $p < 0.05$). Additionally, there may be some modulation of a conductance apart from GIRK channels in all neurons from morphine-treated animals during withdrawal, because the MENK currents that reversed polarity positive of −136 mV did so at significantly more negative potentials than in neurons from vehicle-treated mice (withdrawal, −118.1 ± 2.4, n = 13, versus vehicle, −107.9 ± 2 mV, n = 35; $p < 0.02$). In addition to modulation of another conductance during withdrawal, MENK induced any current in fewer neurons from morphine-treated mice (vehicle, 39 of 42, versus spontaneously withdrawn, 37 of 51 cells; $\chi^2 = 6.34$, $p < 0.05$) and the amplitude of the current was smaller (Figure 2E).

The properties of the additional conductance were determined in isolation by blocking the GIRK channels activated by MENK using $BaCl_2$ (1–3 mM; North and Williams, 1985). When GIRK channels were blocked, MENK (30 μM) did not produce any current in neurons from vehicle-treated mice (Figure 2F, n = 5) but still produced a current in neurons from morphine-treated

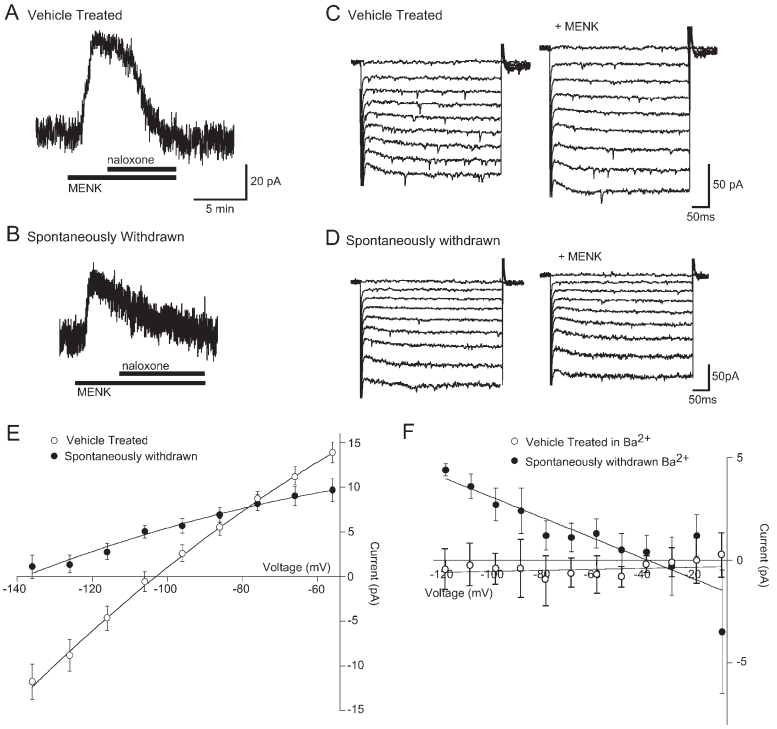

Figure 2. Opioid Receptors Simultaneously Couple to a Potassium Conductance and a Cation Conductance during Spontaneous Withdrawal

(A and B) Example traces of currents from neurons voltage clamped at –56 mV in spontaneously withdrawn slices (drug superfusion shown by bars). MENK (30 μM) induced an outward current that was reversed by naloxone (1 μM) in (A) a vehicle-treated neuron and (B) a neuron from a morphine-treated mouse.

(C and D) Currents produced by voltage steps from –56 mV to –136 mV in –10 mV increments in (C) a vehicle-treated neuron and (D) a neuron from a morphine-treated mouse before (left) and during MENK (30 μM) application (right).

(E) Subtracted current-voltage relationships for MENK (current in MENK – current during control conditions). Reversal potentials were determined at the point where they cross the abscissa. The MENK current reversed polarity near E_k in neurons from vehicle-treated mice (n = 39, open circle), but not in neurons from morphine-treated mice (n = 37, filled circle).

(F) Subtracted current-voltage relationship for MENK (MENK – control) in the modified ACSF (including the addition of Ba^{2+} to block the opioid-activated K^+ current). In Ba^{2+}, MENK failed to produce a current in neurons from vehicle-treated mice (n = 4, open circle), but produced a current that reversed polarity at –40 mV in neurons from morphine-treated mice (n = 4, closed circle).

mice. This current was outward at more negative membrane potentials and reversed polarity at –40 ± 10 mV (Figure 2F, n = 4). This is consistent with previous findings in rat, where the naloxone-induced depolarization produced by withdrawal persisted in Ba^{2+} (Chieng and Christie, 1996). In these experiments, the ACSF was also modified to reduce activation of voltage-activated Ca^{2+} ($CdCl_2$), Na^+ (TTX), and K^+ conductances (TEACl); to reduce neurotransmitter release (0 $CaCl_2$, 10 mM $MgCl_2$); and to shift the reversal potential of mixed-cation conductances to more negative values (lower NaCl, details in Experimental Procedures).

A current that reverses polarity at –40 mV in modified, low-sodium ACSF could be due to MENK-induced activation of a Cl^- conductance or a decrease in the activity of a mixed-cation conductance. The conductance was not a Cl^- conductance, because the reversal potential of the current was 24 mV more positive than E_{Cl} as determined by application of the $GABA_A$ receptor agonist muscimol (3 μM, –64 ± 4 mV in modified ACSF without picrotoxin, n = 4). Therefore, the reversal potential of the additional conductance in the modified ACSF used here is consistent with MENK decreasing the activity of a cation conductance during withdrawal and can be described by a linear "cation" conductance equation with a reversal potential of –40 mV (in modified, low-sodium ACSF, see Experimental Procedures, Equation 1). While the MENK-induced current in neurons from vehicle-treated mice was well modeled by the equation for a GIRK conductance (see Experimental Procedures, Equation 2, R^2 = 0.999), the nonreversing MENK-induced current in neurons from morphine-treated mice was poorly fit by the GIRK equation (R^2 = 0.002). However, it was well modeled by a combination of an increased GIRK and decreased cation conductance, with a reversal potential of –27 mV (calculated E_{rev} for standard, normal sodium ACSF, see Experimental Procedures, Equation 3, R^2 = 0.992). Therefore, the nonreversing current MENK induced in morphine-treated mice can be explained by simultaneous activation of the GIRK conductance and inhibition of a cation conductance.

One candidate for the opioid-sensitive cation conductance is the hyperpolarization activated cation conductance, I_h, which is inhibited by opioids in nodose ganglion (Ingram and Williams, 1994) and hippocampal neurons (Svoboda and Lupica, 1998). A small-amplitude, time-dependent I_h current was observed in PAG neurons from both morphine- and vehicle-treated animals (note the current relaxation at the very negative potentials in Figures 2C and 2D), but the MENK-induced current still failed to reverse polarity if the measurements were taken before I_h was activated (beginning of voltage step, n = 37). Moreover, the reversal potential of the MENK-induced current in morphine-dependent mice was unaffected by the I_h blocker ZD7288 (50 μM), i.e., when I_h was blocked, the current still did not reverse at E_K, and its amplitude at –136 mV was unaffected by ZD72888 (1 ± 3 pA reduction, Figure 3B, n = 4).

Inhibition of GAT-1 Abolishes Opioid Modulation of the Cation Conductance and Withdrawal Hyperexcitation

Acutely opioids inhibit GABA release in the PAG, but one consequence of opioid withdrawal is a rebound increase in synaptic release of GABA (Ingram et al., 1998; Hack et al., 2003). Therefore, we considered

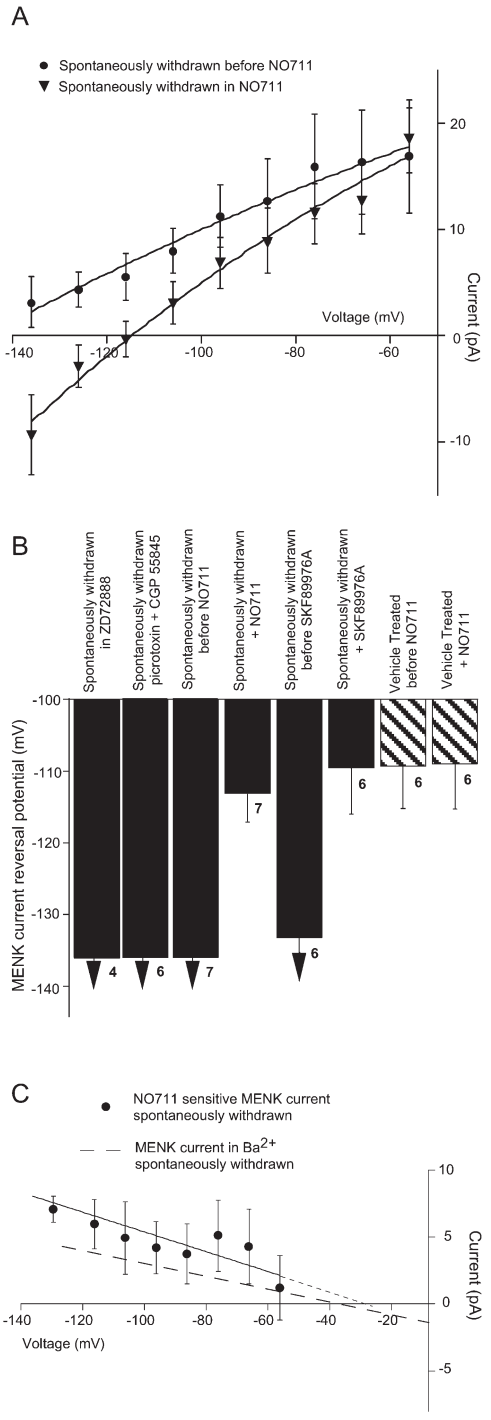

Figure 3. GAT-1 Inhibition Abolished Opioid Modulation of the Cation Conductance

(A) Subtracted current-voltage relationships for MENK (MENK – control). In neurons from morphine-treated animals, MENK currents failed to reverse polarity before addition of the GAT-1 inhibitor NO711 (filled circle), but reversed polarity close to E_K during superfusion of NO711 (10 μM, n = 7, filled triangle).

(B) Reversal potential of the MENK-induced currents before and after addition of GAT-1 inhibitors. In spontaneously withdrawn neurons, the I_h blocker ZD72888 (50 μM) or GABA receptor antagonists (100 μM picrotoxin, 1 μM CGP55845) did not alter the reversal potential of the MENK current, but when GAT-1 was inhibited by NO711 (10 μM) and SKF89976A (10–100 μM), the current reversed polarity close to E_K. Filled bars, spontaneously withdrawn neurons; hatched bars, neurons from vehicle-treated animals. Arrows indicate that the average current did not reverse polarity at the most negative potential that could be tested (–136 mV). The number of neurons is shown below the bars.

(C) Subtracted current-voltage relationship for the MENK current sensitive to NO711 (MENK in morphine-treated – MENK in morphine-treated plus NO711 10 μM, n = 7, filled circles) is similar to the additional MENK-blocked current after morphine treatment (in ACSF modified to block the opioid-activated K^+ current, as shown in Figure 2F, dashed line).

whether the opioid-sensitive cation conductance could be due to a GABA-related conductance. The nonreversing opioid current and increased action potential rate in neurons from morphine-treated mice persisted in the presence of high concentrations of the $GABA_A$ and $GABA_C$ receptor blocker picrotoxin (100 μM) and the $GABA_B$ receptor blocker CGP55845 (1 μM, Figure 3B; CGP55845 was present in all subsequent experiments). Additionally, the current did not reverse polarity close to the reversal potential of GABA receptor currents.

The cation conductance activated by opioid withdrawal could result from GABA transport activity, because the GABA transporter that is expressed in PAG neurons, GAT-1 (Barbaresi et al., 2001), is electrogenic, i.e., GABA transport into neurons results in a net +1 inward charge movement (Mager et al., 1993). Additionally, under some conditions the GAT-1 transporter may also have uncoupled and/or leak conductances (Mager et al., 1993; Cammack and Schwartz, 1996). The selective nontransportable inhibitors of GAT-1, NO711 and SKF 89976A (Suzdak et al., 1992; Borden et al., 1994), both potentiated the currents induced by superfusion of GABA (10 mM, 64 ± 12 pA at –56 mV, n = 8), indicating that they effectively inhibited GAT-1 activity (NO711 [10 μM], 189.6% ± 17% of control, n = 4 and SKF 89976A [100 μM], 135% ± 12%, n = 4). The GABA-induced current was blocked by picrotoxin (100 μM).

Inhibition of GAT-1 with NO711 (10 μM) produced a small outward current (5.9 ± 2.3 pA, n = 5) in neurons from morphine-treated mice but failed to produce any current in neurons from vehicle-treated mice (–1.27 ± 3.6 pA), suggesting that GAT-1 activity is increased during opioid withdrawal. MENK (30 μM) currents in neurons from morphine-treated mice that failed to reverse polarity in the absence of NO711 subsequently reversed polarity close to E_K in the presence of NO711 (10 μM for 10 min; Figures 3A and 3B). Similarly, SKF 89976A (10–100 μM for 10 min) shifted the reversal potential for the MENK-induced current close to E_K (Figure 3B; note that the mean reversal potential for withdrawn PAG neurons before application of SKF 89976A is shown to be less than –136 mV because a reversing current was observed in one of these neurons [E_{rev} = –120 mV]). NO711 and SKF 89976A did not affect the reversal potential in neurons from vehicle-treated mice (Figure 3B).

These results indicate that during opioid withdrawal GAT-1 activity is increased and that when GAT-1 is inhibited MENK reverts to activating a potassium conductance in neurons from morphine-treated mice. The

MENK current that is sensitive to inhibition by NO711 (Figure 3C, normal Na^+ ACSF) had an extrapolated reversal potential of –30 mV, which is similar to that of the GAT-1 current activated by GABA in Bergmann glia (Barakat and Bordey, 2002). The reversal potential of the NO711-sensitive current is 10 mV more positive than that of the conductance inhibited by MENK during opioid withdrawal in the low-Na^+ external solution (Figure 2F, Na [30 mM] replaced with TEA [30 mM]), which is the predicted shift in reversal potential for GAT-1 currents (Lu and Hilgemann, 1999).

Increased GABA Release during Withdrawal Does Not Cause the GAT-1-Mediated Cation Current

Since there is an enhancement of GABA (but not glutamate) release under some conditions during withdrawal (Ingram et al., 1998; Hack et al., 2003), it is possible that the increased GAT-1 activity observed during withdrawal resulted from more transporter substrate. To test whether synaptically released GABA is necessary for activation of the current, we attempted to abolish all release. Recent work has shown that activation of phosphatidylinositol 3-kinase (PI3K) is necessary for the delivery of synaptic vesicles to the readily releasable pool (RRP) after their liberation from the reserve pool (Cousin et al., 2003). Inhibition of PI3K with wortmannin led to enhanced rundown of glutamatergic synaptic transmission during repetitive stimulation in hippocampal neurons (Cousin et al., 2003). To reduce quantal release, slices were preincubated ($\geq$2 hr immediately after dissection) in ACSF containing wortmannin (5 μM) to inhibit replenishment of the RRP and sucrose (50 mM, osmolarity increase from 310 to 360 mOsmoll) to exhaust vesicles already present in the RRP. This pretreatment profoundly reduced the frequency (Figures 4Ai and 4Aii) but not the amplitude (vehicle: 44 ± 4 pA, n = 7, after pretreatment, 40 ± 9 pA, n = 6; spontaneously withdrawn: 57 ± 4.3 pA, n = 10, after pretreatment, 49 ± 8 pA, n = 7) of miniature inhibitory postsynaptic currents (mIPSCs) in slices from both morphine- and vehicle-treated mice for at least 1 hr after the incubation. The ACSF contained CNQX (5 μM), TTX (1 μM), and CGP55845 (1 μM). MENK (30 μM) currents in neurons from morphine-treated mice failed to reverse polarity at the most negative potentials tested (interleaved controls), but after pretreatment to abolish synaptic release, the MENK current reversed polarity close to E_K (Figure 4Aiii). The pretreatment did not affect the reversal potential of MENK currents in neurons from vehicle-treated mice (Figure 4Aiii). Therefore, profoundly reducing release of GABA (and other neurotransmitters) abolishes opioid modulation of the GAT-1 current, indicating that a dramatic reduction in the substrate reduced the activity of the transporter.

Conversely, to test whether increasing neurotransmitter release is able to stimulate the current in untreated mice, we raised extracellular osmolarity. Adding 50 mM sucrose increased the rate of mIPSCs by 100% (Figures 4Bi and 4Bii), which is similar to the increase produced by opioid withdrawal (Ingram et al., 1998; Hack et al. 2003). However, it did not alter the reversal potential of the MENK currents (Figure 4Biii). Increasing extracellular GABA concentration using exogenous GABA also failed to induce the GAT-1-mediated cation current, because the reversal potential of superfused GABA was close to E_{Cl} both in the absence and, when any current was detected, in the presence of TTX, CNQX, bicuculline, picrotoxin, CGP55845, gabazine (20 μM), and strychnine (3 μM) (–69 ± 3 mV, n = 11). Therefore, while some spontaneous neurotransmitter release is required for opioids to modulate the GAT-1 current after chronic morphine treatment, increasing GABA release in control slices or addition of exogenous GABA is not sufficient to cause opioid modulation of GAT-1 or activation of the transporter current.

GAT-1 Protein Expression Is Unchanged by Opioid Withdrawal

Because increasing neurotransmitter release is not sufficient to activate the GAT-1 mediated current, it is possible that the current occurs during withdrawal because there is more GAT-1 protein. To examine this possibility, slices of PAG were taken from control (four mice, 600 μm slice each mouse) and withdrawn mice (five mice) and processed for quantitative immunoblotting for GAT-1 and a loading control, α-actinin. A representative immunoblot for GAT-1 is shown in Figure 5A, and the bar chart summarizes the quantitative analysis of the gray value of bands from all mice: with GAT-1 expressed relative to α-actinin. There was no difference in the absolute level of GAT-1 between vehicle-treated and withdrawn mice (gray value: 135 ± 15 versus 130 ± 11) or the level relative to the loading control protein (Figure 5A).

Although the immunoblots show that the total level of GAT-1 immunoreactivity in the PAG was not altered we also used immunohistochemistry to determine whether chronic opioid treatement altered GAT-1 levels in a subdivision of the PAG. GAT-1 immunoreactivity was concentrated throughout the PAG (Figure 5B) and appeared as a punctate, dense reaction product that surrounded cell bodies and outlined dendrites (Figure 5B, inset) and closely resembled the anatomical pattern of GAT-1 immunoreactivity in the cat PAG (Barbaresi et al., 2001). Electrophysiological recordings were made from ventrolateral PAG neurons. As the terminals of ventrolateral PAG neurons may extend beyond the ventrolateral PAG, we also examined GAT-1 immunoreactivity in the neighboring brain structures. Immunoreactivity for GAT-1 was significantly greater in the lateral PAG and dorsal raphe than in the ventrolateral PAG, but there was no difference in any region of the PAG or dorsal raphe between vehicle-treated and withdrawn mice (Figure 5C). Therefore, as no difference could be detected in the total protein level of GAT-1 in the PAG during spontaneous withdrawal using either Western blots or immunohistochemistry, the additional GAT-1 current is not due to more total GAT-1 protein.

PKA Activity Is Required for Opioid Modulation of the Cation Conductance and Withdrawal Hyperexcitation

The withdrawal-induced GAT-1 cation current could result from the elevated adenylyl cyclase/PKA signaling that develops in PAG during opioid withdrawal (Maldonado et al., 1995; Punch et al., 1997; Williams et al., 2001). If so, the selective, membrane-permeable PKA

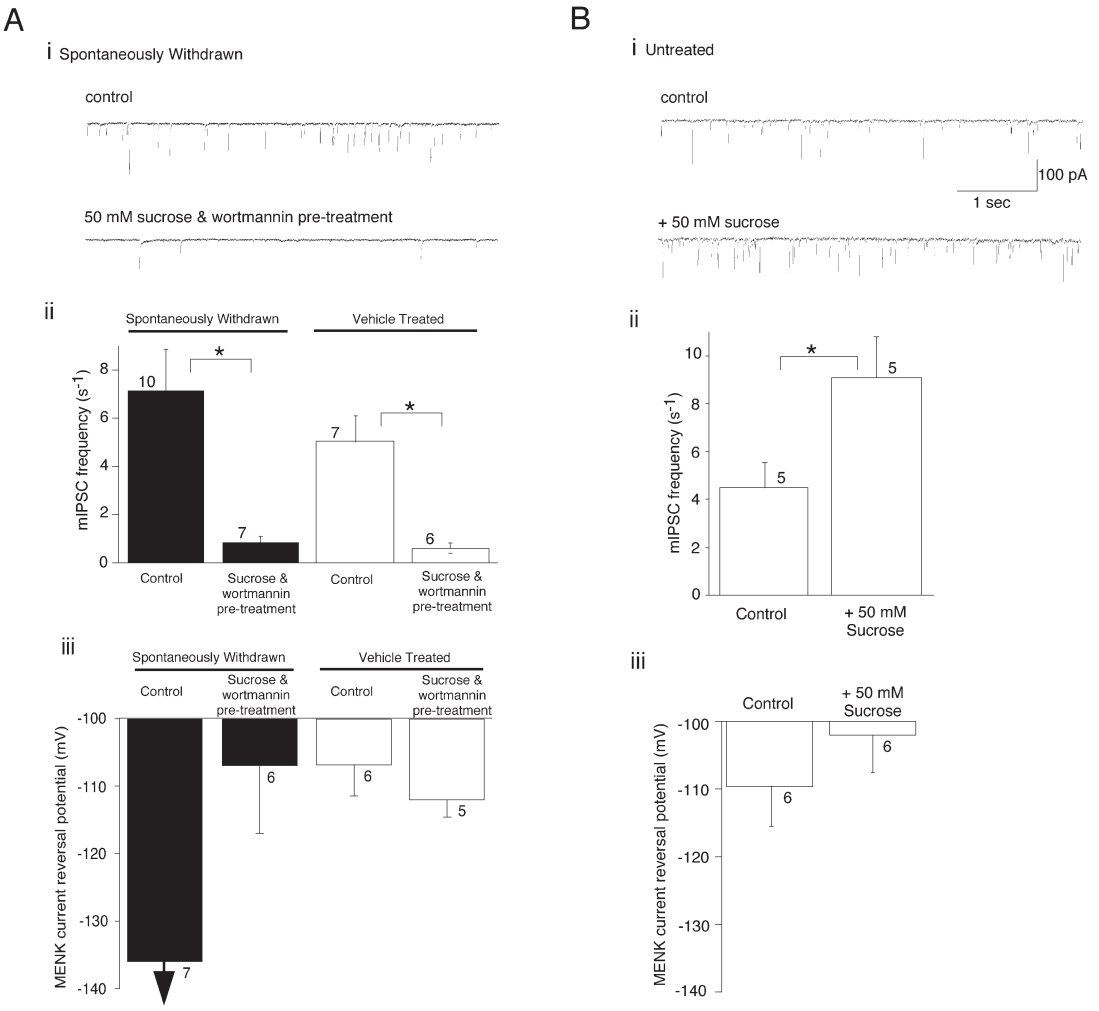

Figure 4. Profound Reduction of Spontaneous mIPSCs in Opioid-Dependent Neurons Abolished Opioid Modulation of the Cation Conductance but Increased GABA Release in Control Neurons Did Not Mimic Opioid Withdrawal

(Ai) Example traces of mIPSCs from a neuron in a spontaneously withdrawn slice. Pretreatment with sucrose and wortmannin to deplete the RRP of synaptic vesicles and prevent entry of vesicles into the RRP profoundly reduced mIPSC frequency. (Aii) Quantification of the mIPSC frequency with or without wortmannin and sucrose pretreatment. Pretreatment significantly reduced the frequency in neurons from vehicle- and morphine-treated mice (*$p < 0.001$). Filled bars, spontaneously withdrawn neurons; open bars, neurons from vehicle-treated mice. The number of neurons is shown above or below the bars. (Aiii) Reversal potential of the MENK-induced currents with or without wortmannin and sucrose pretreatment. After pretreatment, the MENK current in neurons from morphine-treated mice reversed polarity close to E_K. Arrows indicate that the average current did not reverse polarity at the most negative potential that could be tested (–136 mV).

(Bi) Example traces of mIPSCs from a control neuron before and during sucrose. Raising osmolarity by adding sucrose increased the mIPSC frequency. (Bii) Quantification of the mIPSC frequency before or during sucrose. Sucrose (50 mM) significantly increased the frequency of mIPSCs in neurons from control mice (paired Student's t test, *$p < 0.03$). (Biii) Reversal potential of the MENK-induced currents with or without sucrose. High osmolarity did not alter the reversal potential of the MENK current.

inhibitor RP-8-cpt-cAMPS or the nonselective protein kinase inhibitor staurosporine should block the MENK-induced current. MENK (30 μM) currents in neurons from morphine-treated mice that did not reverse polarity prior to RP-8-cpt-cAMPS reversed polarity close to E_K in the presence of RP-8-cpt-cAMPS (100 μM for 10 min; Figures 6A and 6B). Similarly, in cells incubated in staurosporine (1 μM for >1 hr), the current produced by MENK (30 μM) reversed polarity closer to the predicted E_K (Figure 6B). RP-8-cpt-cAMPS did not alter the MENK-induced current in neurons from vehicle-treated mice (Figure 6B). These data suggest that during withdrawal, PKA activation stimulates the activity of GAT-1, and if PKA is inhibited during withdrawal, the stimulation of GAT-1 activity is prevented and MENK reverts to exclusively modulating a GIRK conductance.

Adenylyl Cyclase Activation Mimics Opioid Withdrawal

If induction of the GAT-1 cation current during withdrawal is produced as a result of increased PKA activity, then increasing adenylyl cyclase activity in neurons from untreated mice should mimic the effect of opioid withdrawal in a GAT-1-dependent manner. Increasing

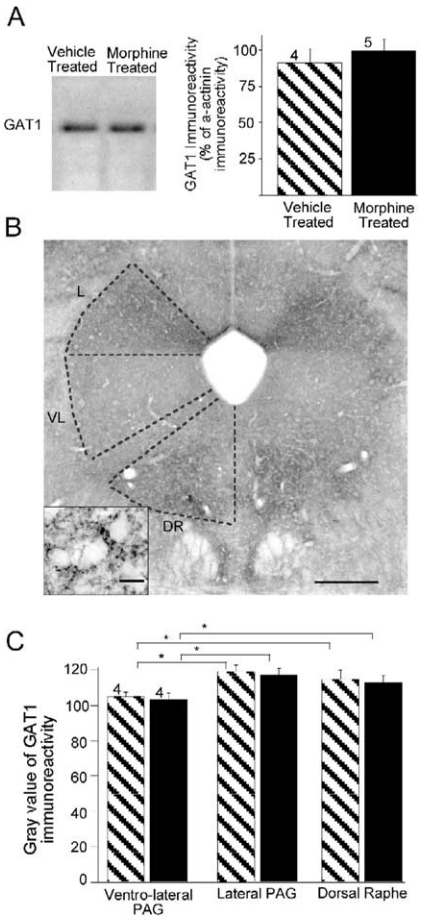

Figure 5. Expression of GAT-1 Is Unchanged in PAG by Opioid Withdrawal

(A) Opioid withdrawal does not alter total GAT-1 immunoreactivity. Example immunoblot showing GAT-1 immunoreactivity in lysates of PAG from vehicle-treated and morphine-treated mice after induction of withdrawal in vivo with naloxone. The graph quantifies GAT-1 immunoreactivity in vehicle- or morphine-treated mice as a percentage of the immunoreactivity for the loading control protein α-actinin. Filled bars, spontaneously withdrawn neurons; hatched bars, neurons from vehicle-treated mice.

(B) GAT-1 immunoreactivity was differentially distributed in different columns of the PAG. Broken lines mark boundaries of the lateral (L), ventrolateral (VL) PAG, and dorsal raphe (DR) nucleus. Inset shows punctate blue/black GAT-1 staining surrounding PAG cells. Scale bars: main, 250 μm; inset, 15 μm.

(C) The graph quantifies the gray value of GAT-1 immunoreactivity. GAT-1 immunoreactivity differed significantly (*$p < 0.05$) among different columns of the PAG, but was not different between vehicle-treated (hatched bars) and morphine-treated mice (filled bars). The number of animals is shown above the bars.

adenylyl cyclase activity using forskolin (10 μM) induced an inward current that was blocked by NO-711 (1 μM) in neurons from vehicle-treated mice (Figure 6C, n = 4), but without PKA activation, NO-711 did not block a current in vehicle-treated mice. Therefore, PKA activation can stimulate a GAT-1 current, and this suggests that opioids modulate a single additional conductance during withdrawal that relies on PKA and is due to activity of GAT-1. The inward current had a reversal potential of –39 mV ± 10 mV (in modified, low-sodium ACSF; Figure 6D, n = 7), which is both consistent with activation of a cation conductance and very close to the reversal potential of the cation conductance inhibited by MENK in low-sodium ACSF during opioid withdrawal (Figure 2F). Dideoxyforskolin (10 μM), an analog of forskolin that does not activate adenylyl cyclase, did not induce an inward current (dideoxyforskolin, –0.5 ± 1.7 pA, n = 4, versus forskolin, –9.5 ± 4.2 pA, n = 4 at –110 mV).

MENK (30 μM) currents in neurons from untreated mice that reversed polarity close to E_K prior to application of forskolin no longer reversed polarity at the most negative potential tested (–136 mV) in the presence of forskolin (10 μM for 10 min, n = 6, Figure 6B). After activation of a cation conductance by forskolin, the MENK current in neurons from untreated mice resembled the MENK current in neurons from morphine-treated mice (Figure 2E). In both cases, the extrapolated reversal potential of the additional cation current was close to –30 mV (normal sodium ACSF). Therefore, the GAT-1-mediated, opioid-sensitive cation conductance can be prevented by inhibition of PKA activity in morphine-dependent PAG neurons and rapidly stimulated by activation of adenylyl cyclase in neurons from untreated animals. These results suggest that chronic opioid treatment increases the activity of the adenylyl cyclase cascade and that removal of opioid inhibition (i.e., withdrawal) relieves inhibition of adenylyl cyclase and allows activation of the GAT-1 conductance. Readdition of opioid agonists (MENK) inhibits the conductance via inhibition of adenylyl cyclase activity.

PKA-Dependent Activation of the GAT-1 Cation Conductance Mediates Hyperexcitation of PAG Neurons during Withdrawal

Although the opioid-sensitive GAT-1 current in morphine-treated mice was small (Figure 3C; 3 pA at –56 mV), because the input resistance of mouse PAG neurons was high (1.83 ± 0.32 GΩ, –60 to –70 mV, n = 92) this current would still be expected to depolarize the neurons by approximately 5.5 mV. This depolarization could be sufficient to produce the increased action potential rate observed during opioid withdrawal, so we tested whether preventing activation of the cation conductance by inhibiting GAT-1 or PKA reduced the naloxone-precipitated withdrawal stimulation of action potential rate in morphine-treated mice.

When all GABA receptors were blocked, synaptic transmission blockers were present, and slices maintained in morphine (5 μM), the addition of naloxone (1 μM) produced a significantly larger increase in action potential rate in neurons from morphine-treated mice than in neurons from vehicle-treated mice (Figure 7A). By contrast, in NO711 (10 μM for 10 min), the naloxone-induced increase in action potential rate of neurons from morphine-treated mice was similar to the increase in neurons from vehicle-treated mice (Figure 7A). NO711 did not affect the smaller response to naloxone in vehicle-treated neurons (Figure 7A). These results suggest that inhibition of GAT-1 prevents opioid modulation of the cation conductance activated during opioid withdrawal and this prevents the increase in action potential rate produced by opioid withdrawal.

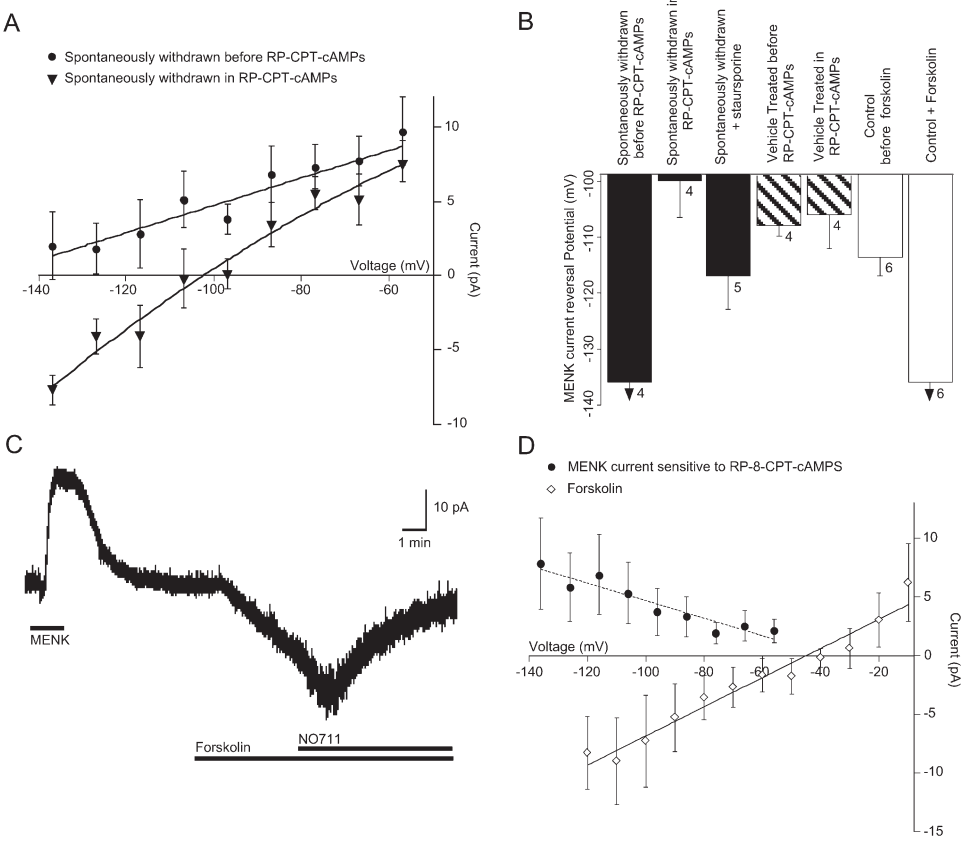

Figure 6. Opioid Modulation of the GAT-1 Conductance Depends on Activation of PKA

(A) Current-voltage relationships for MENK (30 μM, MENK – control). In neurons from morphine-treated animals MENK currents failed to reverse polarity before addition of the PKA inhibitor RP-CPT-cAMPs (filled circle) but reversed polarity close to E_K during superfusion of RP-CPT-cAMPs (100 μM, n = 4, filled triangle).

(B) Reversal potential of the MENK-induced currents before and during modulation of PKA activity. When PKA was inhibited by RP-CPT-cAMPs (100 μM) or staurosporine (1 μM) in spontaneously withdrawn neurons the MENK current reversed polarity close to E_k. In neurons from control mice, activation of PKA, using forskolin (10 μM), mimics opioid withdrawal, as the MENK current no longer reverses polarity. Filled bars, spontaneously withdrawn neurons; hatched bars, neurons from vehicle-treated mice; open bar, neurons from control mice. Arrows indicate that the average current did not reverse polarity at the most negative potential that could be tested (–136 mV). The number of neurons is shown below the bars.

(C) Example trace of currents from a neuron whole-cell voltage clamped at –56 mV (drug superfusion shown by bars). In a neuron sensitive to MENK (30 μM), forskolin (10 μM) induced an inward current in a neuron from an untreated mouse that is inhibited during superfusion of the GAT-1 inhibitor NO711 (10 μM).

(D) Subtracted current-voltage relationship for MENK current sensitive to RP-CPT-cAMPs (MENK before RP-CPT-cAMPS – MENK in RP-CPT-cAMPs, 100 μM, n = 5, filled circle) in neurons from morphine-treated mice and the forskolin-induced current in neurons from untreated mice (forskolin – control, 10 μM, n = 7, open diamond).

The hyperexcitation of PAG neurons during withdrawal was also blocked by PKA inhibitors. When slices from dependent mice were maintained in morphine (5 μM) and superfused with RP-CPT-cAMPs (100 μM for 10 min), subsequent naloxone (1 μM) cosuperfusion no longer produced a greater increase in action potential rate than in vehicle-treated mice (Figure 7B). RP-CPT-cAMPs did not affect the naloxone response in neurons from vehicle-treated mice (Figure 7B). Therefore, PKA activity during opioid withdrawal is necessary for both activation of the GAT-1 cation conductance and the increased action potential frequency.

Discussion

During opioid withdrawal, opioid-sensitive PAG neurons fire action potentials more frequently than neurons from control animals (Chieng and Christie, 1996). In this study, we have shown that opioid withdrawal activates an opioid-sensitive cation current that is dependent on PKA activity and is due to GAT-1 activity. When activation of this current is prevented by inhibition of PKA or GAT-1, the elevated action potential rate of PAG neurons during withdrawal is also prevented. The present results provide direct experimental evidence supporting the suggestion that enhanced PKA signaling causes the increase in neuronal action potential rate during opioid withdrawal (Kogan et al., 1992; Chieng and Christie, 1996; Nestler et al., 1999; Ivanov and Aston-Jones, 2001) and identify the underlying ionic mechanism.

The fact that opioid withdrawal increased the action potential rate of PAG neurons through GAT-1 was unexpected. While there are many examples of indirect ac-

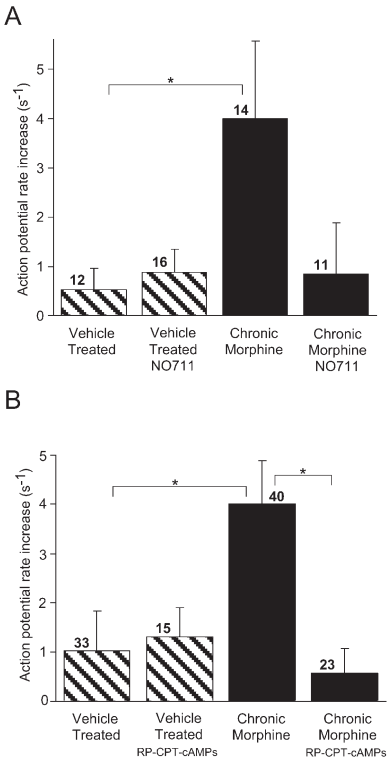

Figure 7. Inhibition of GAT-1 or PKA Prevents Hyperexcitation of Action Potential Frequency during Opioid Withdrawal

(A) The increase in action potential rate induced by naloxone was significantly greater in neurons from morphine-treated than vehicle-treated mice (*$p < 0.05$). GAT-1 inhibition by NO711 (10 μM) abolished the increased action potential rate during withdrawal in neurons from morphine-treated mice but had no effect on the increase in action potential rate induced by naloxone in neurons from vehicle-treated mice. Filled bars, spontaneously withdrawn neurons; hatched bars, neurons from vehicle-treated mice. The number of neurons is shown above the bars.

(B) The naloxone-induced increase in action potential rate was significantly greater in neurons from morphine-treated than vehicle-treated mice (*$p < 0.05$). PKA inhibition by RP-CPT-cAMPS (100 μM) abolished the increased action potential rate during withdrawal in neurons from morphine-treated mice (*$p < 0.05$) but had no effect on the increase in action potential rate induced by naloxone in neurons from vehicle-treated mice.

tions of GAT-1 inhibitors resulting from increased extracellular GABA (e.g., Isaacson et al., 1993), a direct effect of GAT-1 currents on action potential rate has not been shown. In fact, only dopamine transporter currents have been shown to directly alter neuron action potential rate (Ingram et al., 2002). An elevated action potential rate or depolarization due to activation of GAT-1 might be predicted by the inward current induced by activating GABA transporters in horizontal retinal cells (Malchow and Ripps, 1990; Cammack and Schwartz, 1993) or GAT-1 in Bergmann glia (Barakat and Bordey, 2002). An indirect effect of GAT-1 inhibition is unlikely to account for the block of the cation conductance and the increased action potential rate observed in this study, as all GABA receptors were blocked and the reversal potential of the current was distinct from the reversal potential of GABA receptor currents.

The reversal potential and direction of ion flux of the cation current were similar to those of the cloned GAT-1 transporter (Risso et al., 1996) and pharmacologically defined GAT-1 conductances in Bergman glia (Barakat and Bordey, 2002). The reversal potential of the cation conductance could reflect reversal of the transporter or the activity of a nonstoichiometric GAT-1 current. It is possible that this reflects transport reversal because it is likely that physiological levels of intracellular GABA were maintained in the perforated patch recording configuration, which are the conditions previously shown to be required to observe transport reversal (Cammack and Schwartz, 1993; Risso et al., 1996; Barakat and Bordey, 2002). NO-711 and SKF-89976A are highly selective for GAT-1 among the four cloned GABA transporters (Suzdak et al., 1992; Borden et al., 1994), and at the concentrations used in this study, other nonspecific effects of NO711 and SKF-89976A are unknown; no effects were detected in neurons from vehicle-treated mice. Additionally, NO711 lacks affinity for many other transporters, ion channels, and receptors—specifically the μ- and κ-opioid receptors (Suzdak et al., 1992). Supporting the involvement of GAT-1, the presence of some substrate was necessary for the transporter to be active, as a dramatic reduction of vesicular GABA release prevented opioid modulation of the current.

As in other brain regions, GAT-1 immunoreactivity was detected in PAG neurons that were mainly (although not exclusively) thought to be GABAergic interneurons based on anatomical criteria (Barbaresi et al., 2001). It is likely that the neurons in which we observed the opioid-sensitive cation current and the increased excitability were GABAergic neurons, as many PAG neurons express immunoreactivity for both GABA and the μ-opioid receptor (Kalyuzhny and Wessendorf, 1998). Further, neurons which express c-Fos immunoreactivity (a marker for raised neuronal activity) during opioid withdrawal are likely to be GABAergic interneurons, as they do not project to the rostral ventromedial medulla (Bellchambers et al., 1998). Therefore, the additional conductance modulated by opioids during withdrawal from chronic opioids was qualitatively similar to GAT-1, blocked by GAT-1 inhibitors, prevented when GABA release was almost abolished, and likely occurred in GABAergic neurons.

The opioid-sensitive cation conductance described in this study relies on intact PKA signaling. It is unlikely that PKA phosphorylation directly modifies GAT-1 activity, as the only consensus site for PKA phosphorylation is extracellular (Guastella et al., 1990). The effect of activation of PKA on the GAT-1 transporter has not been comprehensively studied, but the subcellular location, enzymatic activity, and absolute level of GAT-1 is regulated in a complex inter-related manner by PKC activity, GABA concentration, ionic conditions, tyrosine kinase activity, and the release protein syntaxin 1A (Beckman et al., 1998; Beckman and Quick, 1998; Whitworth and Quick, 2001; Quick, 2002). It is possible that PKA indirectly modifies the transporter activity through one of these regulatory mechanisms. Indeed, PKA stimulation indirectly increases GABA transporter activity in the striatum, and morphine reduces this stimulated activity (Schoffelmeer et al., 2000). Acute stimulation of adenylyl cyclase in control PAG neurons was able to activate the cation conductance, suggesting that GAT-1

can be acutely regulated by adenylyl cyclase activity. Since there is a rebound PKA-dependent enhancement of GABA release during withdrawal (Ingram et al., 1998) and stimulating adenylyl cyclase also increases GABA release in untreated animals, we considered the possibility that increased GAT-1 activity observed during withdrawal results from PKA stimulating GABA release, thus providing more transporter substrate. However, increasing GABA release or adding exogenous GABA in control animals did not produce a detectable GAT-1 current or produce opioid modulation of a non-GIRK current. Therefore, increased substrate concentration alone was not sufficient to allow activation of GAT-1. As the total protein level of GAT-1 is not altered after chronic opioid treatment, this indicates that the increased GAT current during withdrawal was not due to an increase in the total number of GAT-1. Indeed, the rapid increase in GAT-1 current with PKA stimulation in control animals is inconsistent with synthesis of new proteins, but it is possible that PKA activation increases the GAT-1 current by translocating the transporters to the cell surface. PKA activity could relocate transporters to the cell surface because PKA phosphorylates and alters the interaction of proteins that bind to syntaxin-1 (Evans et al., 2001; Boczan et al., 2004). Syntaxin-1 directly interacts with GAT-1, and this interaction regulates the level of GAT-1 on the cell surface (Deken et al., 2000).

The withdrawal signs mediated by the PAG are prevented by inhibition of PKA activity in the PAG (Maldonado et al., 1995; Punch et al., 1997). Therefore, it is likely that the GAT-1 depolarizing current that results in increased action potential rate together with increased GABA release probability (Ingram et al., 1998) are the mechanisms underlying the PKA-sensitive withdrawal behaviors mediated by the PAG. It has been proposed that GABAergic inhibition of PAG projection neurons to the medulla during opioid withdrawal ultimately results in the expression of physical signs of withdrawal (Chieng and Christie, 1996). The activation of the GAT-1 current and increased action potential rate shown here would be expected to increase GABA release and thereby inhibit PAG projection neurons. Therefore, through GAT-1 inhibition it might prove possible to selectively inhibit the expression of opioid withdrawal by preventing PAG neuronal hyperexcitability.

Neurotransmitter transporters may be a new family of proteins whose activity is altered as a result of chronic opioid treatment. It is possible that the adaptations described here as well as other modifications of neurotransmitter transporter activity may also occur in brain regions where increased PKA signaling (Terwilliger et al., 1991) or neuronal hyperexcitability has been observed (Baraban et al., 1995; Haghparast et al., 1998). Several studies have shown that glutamate transporter levels are altered by chronic opioid treatment (Ozawa et al., 2001; Mao et al., 2002), suggesting that neurotransmitter transporters may prove to be useful targets for management of opioid dependence. GAT-1 transport inhibitors are currently used to treat epilepsy and are thought to reduce seizures by increasing the extracellular GABA concentration. Our data indicates that under certain conditions GAT-1 currents induce hyperexcitability of central neurons, suggesting that GAT-1 inhibitors could produce their theurapeutic effect through altering extracellular GABA concentrations as well as directly altering the excitability of GABAergic neurons.

Experimental Procedures

Chronic Treatment with Morphine

Morphine dependence was induced by a series of subcutaneous injections of sustained-release morphine suspension into male C57B16/J mice (300 mg/kg morphine base). Injections (0.1–0.2 ml) were made under light halothane anesthesia on days 1, 3, and 5, and mice were used for experiments on days 6 or 7. Morphine base was suspended in 0.1 ml mannide mono-oleate (Arlacel A, Sigma), 0.4 ml light liquid paraffin and 0.5 ml 0.9% w/v NaCl in water. Vehicle-treated mice were injected on the same schedule with morphine-free suspension.

Tissue Preparation and Recordings

PAG slices (220–250 μm) were cut from 4- to 6-week-old mice and were maintained at 34°C in a submerged chamber containing physiological saline (ACSF) equilibrated with 95% O_2 and 5% CO_2 and were later transferred to a chamber superfused at 2 ml/min with ACSF (34°C) for recording. The standard ACSF contained 126 mM NaCl, 2.5 mM KCl, 1.4 mM NaH_2PO_4, 1.2 mM $MgCl_2$, 2.4 mM $CaCl_2$, 11 mM glucose, and 25 mM $NaHCO_3$. The modified ACSF contained 96 mM NaCl, 30 mM TEACl, 5 mM HEPES, 2.5 mM KCl, 0 mM NaH_2PO_4, 10 mM $MgCl_2$, 0 mM $CaCl_2$, 5 mM $NaHCO_3$, 11 mM glucose, 0.01 mM $CdCl_2$, and 0.0003 mM tetrodotoxin. Brain slices from both morphine-dependent and vehicle-treated mice were maintained in vitro in ACSF containing 5 μM morphine. Unless otherwise stated, slices were spontaneously withdrawn by incubation in morphine-free ACSF for at least 1 hr before an experiment. CGP55845 was a gift from Ciba Ltd (Basel, Switzerland).

PAG neurons were visualized using infra-red Nomarski optics. Perforated patch recordings were made using patch electrodes (4–5 mΩ) filled with 120 mM K acetate, 40 mM HEPES, 10 mM EGTA, 5 mM $MgCl_2$, with 0.25 mg/ml Pluronic F-127, 0.12 mg/ml amphotericin B (pH 7.2, 290 mosmol/l). Liquid junction potentials for K acetate internal solution of –8 mV with ACSF and –12 mV with modified ACSF were corrected. Series resistance (<25 MΩ) was compensated by 80% and continuously monitored. During perforated patch recordings, currents were recorded using a Axopatch 200A amplifier (Axon Instruments), digitized, filtered (at 2 kHz), and then acquired (sampling at 10 kHz) in pClamp (Axon Instruments) or using Axograph Acquisition software (Axon Instruments).

Equations

Current-voltage curves were fit to the experimental data using the following equations.

The additional MENK-induced current in morphine-dependent mouse neurons (Figure 2F) was fit with a curve described by the equation

$$I_{CAT} = g_{CAT(max)}(V - E_{CAT(rev)}). \quad (1)$$

Using this equation, it was found that $g_{CAT(max)}$ = –0.1 nS and that $E_{CAT(rev)}$ = –40 mV (low sodium).

The MENK-induced current in neurons from vehicle-treated mice was fit with a GIRK conductance equation (Shen and North, 1992):

$$I_{K,IR} = g_{k,IR(max)} \times (V - E_{K,IR}) / [1 + \exp((V - E_{K,IR}) / \text{factor})]. \quad (2)$$

Where the factor takes into account the inward rectification of the potassium conductance. For control neurons (Figure 2E) it was found that $g_{k,IR}$ = 0.7 nS, $E_{k,IR}$ = –103 mV, and factor = 169.

The MENK-induced current in neurons from morphine-dependent mice (Figure 2E) was fit with a combination of the GIRK conductance Equation 2 minus a cation conductance Equation 1:

$$\text{combination} = g_{k,IR(max)} \times (V - E_{K,IR}) / [1 + \exp((V - E_{K,IR}) / \text{factor})] - g_{CAT(max)}(V - E_{CAT(rev)}). \quad (3)$$

From Equation 2, $E_{K,IR}$ was set at –103 mV, factor 169, and $E_{CAT(rev)}$ =

–27 mV (calculated $E_{CAT(rev)}$ for normal sodium conditions). It was found that $g_{k,IR(max)}$ = 0.4 nS and $g_{CAT(max)}$ = 0.1 nS.

Cell-attached recordings were made using patch electrodes (4–5 MΩ) filled with K acetate solution, as above, but excluding pluronic acid and amphotericin B. During cell-attached recordings, capacitative action potentials were measured in voltage-clamp without an applied command potential and were either recorded on video tape (via Vetter PCM) and then later digitized offline in Fetchex (sampling at 5 kHz) or acquired using Axograph. After the cell-attached recording was completed, suction was applied to establish whole-cell current clamp recording to measure resting membrane potential (RMP) and amplitude of action potentials. Neurons were excluded from further analyses if the RMP was more positive than –45 mV or if the action potential amplitude was less than 50 mV. Data were then analyzed offline using Axograph. The increase in action potential rate was calculated by subtracting the 3 min preceding naloxone from the last 2 min of naloxone.

To record $GABA_A$ mIPSCs, whole-cell voltage clamp recordings were made using patch electrodes (2–5 MΩ) containing 140 mM CsCl, 10 mM EGTA, 5 mM HEPES, 2 mM $CaCl_2$, and 2 mM MgATP (pH 7.3, 270–290 mOsmol/l). Neurons were voltage clamped to –60 mV, and the series resistance ($\leq$12 MΩ) was compensated by 80% and continuously monitored during experiments. IPSCs were filtered (1 kHz low-pass filter) and sampled at 5 kHz for online and later offline analysis using Axograph 4.8. mIPSCs above a preset threshold (4–5 standard deviations above baseline noise) were automatically detected by a sliding template algorithm, then were manually checked offline.

SDS Page and Immunoblot

Ten minutes after withdrawal was induced by intraperitoneal injection of Naloxone (5 mg/kg), brain slices were cut. Finely chopped PAG slices were homogenized and then lysed in ice-cold RIPA buffer (1% Igepal, 0.5% Na Deoxycholate, 0.1% SDS in phosphate-buffered saline [PBS]) with complete protease inhibitor (1:100, Sigma) for 30 min. Homogenates were spun at 10,000 × g for 10 min at 4°C, and the supernatant protein concentration was determined (Bio-Rad Protein Assay). Sample supernatants (equivalent protein amounts) were loaded on 10% gel (PAGEr Precast Gels, Cambrex) and run at 125 V for 1 hr. Gels were transferred to Immuno-blot PVDF membrane (Bio-Rad) at 100 V for 1 hr, and the membranes were then blocked in 5% milk, 0.05% Tween 20 in Tris-buffered saline (TBS) for 1 hr at room temp. Membranes were cut and then incubated in either rabbit anti-GAT1 (1:500, Cat AB1570W, Chemicon) or mouse anti-α-actinin (1:500, Upstate) for 1 hr at room temp. After washing in TBS, the membranes were incubated in either HRP-conjugated goat anti-rabbit or goat anti-mouse IgG (1:2000, Santa Cruz Biotechnology) for 1 hr at room temp. Membranes were washed in TBS, and the activity of HRP conjugates was determined using chemiluminescence (Biowest Extended Duration Chemiluminescent Substrate) and film (Kodak Biomax light). Immunolabeled bands were identified by their molecular weight and quantified by densitometry (ImageJ 1.32, NIH).

Immunohistochemistry

Ten minutess after withdrawal was induced by intraperitoneal injection of Naloxone (5 mg/kg), mice were anaesthetised with Ketamine hydrochloride and Xylazine hydrochloride and were transcardially perfused with heparinized normal saline (10,000 IU/ml) followed by cold 4% paraformaldehyde in 0.1 M phosphate buffer. Brains were removed, postfixed in the same fixative for 4 hr at 4°C, and then cryoprotected in 30% sucrose in PBS for 48 hr at 4°C. Coronal sections (40 μm) were cut through the PAG using a cryostat. Free-floating sections were washed in PBS and incubated in 50% ethanol and 3% H_2O_2 in water for 20 min. After washing and blocking with 20% normal horse serum (NHS) for 20 min, the sections were incubated in rabbit anti-GAT-1 (1:250, Cat AB1570, Chemicon) with 5% NHS and 0.3% Triton X-100 for 14 hr at room temp. After washing, sections were incubated in biotinylated donkey anti-rabbit IgG (1:500, Amersham) with 2% NHS for 3.5 hr at room temp, washed, and then incubated in HRP conjugated ExtrAvidin (1:1000, Sigma) for 3.5 hr at room temperature. Sections were processed for HRP histochemistry using nickel enhanced DAB as the chromogen and glucose oxidase as the catalyst, which results in a blue/black reaction product. All sections were processed together using the same protocol, solutions, and antibody mixes. Digitized images of the caudal PAG were captured on a light microscope with a high-resolution CCD camera, and ImageJ 1.32 was used to quantify immunoreactivity using densitometry. The mean gray value (MGV) of each region was measured in four sections from each animal, and the average MGV from the four sections was the result for the animal. The MGV of an unlabeled region of the slice was subtracted to reduce background.

All experiments were approved by the Royal North Shore Hospital/University of Technology Sydney Ethics committee. All pooled data are expressed as mean ± SEM. Unless otherwise stated, we tested for significance using the unpaired Student's t test.

Acknowledgments

This work was supported by National Institute on Drug Abuse DA12926-01 (M.J.C and E.E.B.), National Health and Medical Research Council of Australia; C.J. Martin Fellowship (E.E.B), and project grant 153844 (C.W.V). We thank Mark Connor, Susan Ingram, Billy Chieng, and Gary Westbrook for helpful discussions concerning this manuscript.

Received: September 8, 2004
Revised: December 10, 2004
Accepted: December 17, 2004
Published: February 2, 2005

References

Avidor-Reiss, T., Nevo, I., Saya, D., Bayewitch, M., and Vogel, Z. (1997). Opiate-induced adenylyl cyclase superactivation is isozyme-specific. J. Biol. Chem. *272*, 5040–5047.

Baraban, S.C., Stornetta, R.L., and Guyenet, P.G. (1995). Effects of morphine and morphine withdrawal on adrenergic neurons of the rat rostral ventrolateral medulla. Brain Res. *676*, 245–257.

Barakat, L., and Bordey, A. (2002). GAT-1 and reversible GABA transport in Bergmann glia in slices. J. Neurophysiol. *88*, 1407–1419.

Barbaresi, P., Gazzanelli, G., and Malatesta, M. (2001). γ-aminobutyric acid transporters in the cat periaqueductal gray: a light and electron microscopic immunocytochemical study. J. Comp. Neurol. *429*, 337–354.

Beckman, M.L., and Quick, M.W. (1998). Neurotransmitter transporters: Regulators of function and functional regulation. J. Membr. Biol. *164*, 1–10.

Beckman, M.L., Bernstein, E.M., and Quick, M.W. (1998). Protein kinase C regulates the interaction between a GABA transporter and syntaxin 1A. J. Neurosci. *18*, 6103–6112.

Bellchambers, C.E., Chieng, B., Keay, K.A., and Christie, M.J. (1998). Opioid withdrawal and swim-stress increase expression of c-fos immunoreactivity in distinct populations of rat periaqueductal gray neurones. Neuroscience *83*, 517–524.

Boczan, J., Leenders, A.G., and Sheng, Z.H. (2004). Phosphorylation of syntaphilin by cAMP-dependent protein kinase modulates its interaction with syntaxin-1 and annuls its inhibitory effect on vesicle exocytosis. J. Biol. Chem. *279*, 18911–18919.

Borden, L.A., Murali Dhar, T.G., Smith, K.E., Weinshank, R.L., Branchek, T.A., and Gluchowski, C. (1994). Tiagabine, SK and F 89976-A, CI-966, and NNC-711 are selective for the cloned GABA transporter GAT-1. Eur. J. Pharmacol. *269*, 219–224.

Bozarth, M.A., and Wise, R.A. (1984). Anatomically distinct opiate receptor fields mediate reward and physical dependence. Science *224*, 516–517.

Cammack, J.N., and Schwartz, E.A. (1993). Ions required for the electrogenic transport of GABA by horizontal cells of the catfish retina. J. Physiol. *472*, 81–102.

Cammack, J.N., and Schwartz, E.A. (1996). Channel behavior in a γ-aminobutyrate transporter. Proc. Natl. Acad. Sci. USA *93*, 723–727.

Chieng, B., and Christie, M.J. (1994). Hyperpolarization by opioids acting on μ-receptors of a sub-population of rat periaqueductal gray neurones in vitro. Br. J. Pharmacol. *113*, 121–128.

Chieng, B., and Christie, M.J. (1996). Local opioid withdrawal in rat single periaqueductal gray neurons in vitro. J. Neurosci. *16*, 7128–7136.

Collier, H.O., and Roy, A.C. (1974). Morphine-like drugs inhibit the stimulation by E prostaglandins of cyclic AMP formation by rat brain homogenate. Nature *248*, 24–27.

Cousin, M.A., Malladi, C.S., Tan, T.C., Raymond, C.R., Smillie, K.J., and Robinson, P.J. (2003). Synapsin I-associated phosphatidylinositol 3-kinase mediates synaptic vesicle delivery to the readily releasable pool. J. Biol. Chem. *278*, 29065–29071.

Deken, S.L., Beckman, M.L., Boos, L., and Quick, M.W. (2000). Transport rates of GABA transporters: regulation by the N-terminal domain and syntaxin 1A. Nat. Neurosci. *3*, 998–1003.

Evans, G.J., Wilkinson, M.C., Graham, M.E., Turner, K.M., Chamberlain, L.H., Burgoyne, R.D., and Morgan, A. (2001). Phosphorylation of cysteine string protein by protein kinase A. Implications for the modulation of exocytosis. J. Biol. Chem. *276*, 47877–47885.

Fedynyshyn, J.P., and Lee, N.M. (1989). μ type opioid receptors in rat periaqueductal gray-enriched P_2 membrane are coupled to G-protein-mediated inhibition of adenylyl cyclase. FEBS Lett. *253*, 23–27.

Guastella, J., Nelson, N., Nelson, H., Czyzyk, L., Keynan, S., Miedel, M.C., Davidson, N., Lester, H.A., and Kanner, B.I. (1990). Cloning and expression of a rat brain GABA transporter. Nature *249*, 1303–1306.

Hack, S.P., Vaughan, C.W., and Christie, M.J. (2003). Modulation of GABA release during morphine withdrawal in midbrain neurons *in vitro*. Neuropharmacology *45*, 575–584.

Haghparast, A., Semnanian, S., and Fathollahi, Y. (1998). Morphine tolerance and dependence in the nucleus paragigantocellularis: single unit recording study in vivo. Brain Res. *814*, 71–77.

Himmelsbach, C.K. (1943). With reference to physical dependence. Fed. Proc. *2*, 201–203.

Ingram, S.L., and Williams, J.T. (1994). Opioid inhibition of I_h via adenylyl cyclase. Neuron *13*, 179–186.

Ingram, S.L., Vaughan, C.W., Bagley, E.E., Connor, M., and Christie, M.J. (1998). Enhanced opioid efficacy in opioid dependence is caused by an altered signal transduction pathway. J. Neurosci. *18*, 10269–10276.

Ingram, S.L., Prasad, B.M., and Amara, S.G. (2002). Dopamine transporter-mediated conductances increase excitability of midbrain dopamine neurons. Nat. Neurosci. *5*, 971–978.

Isaacson, J.S., Solis, J.M., and Nicoll, R.A. (1993). Local and diffuse synaptic actions of GABA in the hippocampus. Neuron *10*, 165–175.

Ivanov, A., and Aston-Jones, G. (2001). Local opiate withdrawal in locus coeruleus neurons in vitro. J. Neurophysiol. *85*, 2388–2397.

Kalyuzhny, A.E., and Wessendorf, M.W. (1998). Relationship of μ- and κ-opioid receptors to GABAergic neurons in the central nervous system, including antinociceptive brainstem circuits. J. Comp. Neurol. *392*, 528–547.

Kogan, T.A., Nestler, E.J., and Aghajanian, G.K. (1992). Elevated basal firing rates and enhanced responses to 8-Br-cAMP in locus coeruleus neurons in brain slices from opiate-dependent rats. Eur. J. Pharmacol. *211*, 47–58.

Lu, C.C., and Hilgemann, D.W. (1999). GAT1 (GABA:Na+:Cl-) cotransport function. Steady state studies in giant Xenopus oocyte membrane patches. J. Gen. Physiol. *114*, 429–444.

Mager, S., Naeve, J., Quick, M., Labarca, C., and Davidson, N. (1993). Steady states, charge movements, and rates for a cloned GABA transporter expressed in xenopus oocytes. Neuron *10*, 177–188.

Malchow, R.P., and Ripps, H. (1990). Effects of γ-aminobutyric acid on skate retinal horizontal cells: evidence for an electrogenic uptake mechanism. Proc. Natl. Acad. Sci. USA *87*, 8945–8949.

Maldonado, R., Valverde, O., Garbay, C., and Roques, B.P. (1995). Protein kinases in the locus coeruleus and periaqueductal gray matter are involved in the expression of opiate withdrawal. Naunyn Schmiedebergs Arch. Pharmacol. *352*, 565–575.

Mao, J., Sung, B., Ji, R.R., and Lim, G. (2002). Chronic morphine induces down regulation of spinal glutamate transporters: implications in morphine tolerance and abnormal pain sensitivity. J. Neurosci. *22*, 8312–8323.

Mattick, R.P., and Hall, W. (1996). Are detoxification programs effective? Lancet *347*, 97–100.

Nestler, E.J., and Tallman, J.F. (1988). Chronic morphine treatment increases cyclic AMP-dependent protein kinase activity in the rat locus coeruleus. Mol. Pharmacol. *33*, 127–132.

Nestler, E.J., Alreja, M., and Aghajanian, G.K. (1999). Molecular control of locus coeruleus neurotransmission. Biol. Psychiatry *46*, 1131–1139.

North, R.A., and Williams, J.T. (1985). On the potassium conductance increased by opioids in rat locus coeruleus neurones. J. Physiol. *364*, 265–280.

Osborne, P.B., Vaughan, C.W., Wilson, H.I., and Christie, M.J. (1996). Opioid inhibition of rat periaqueductal grey neurones with identified projections to rostral ventromedial medulla in vitro. J. Physiol. *490*, 383–389.

Ozawa, T., Nakagawa, T., Shige, K., Minami, M., and Satoh, M. (2001). Changes in expression of glial glutamate transporters in the rat brain accompanied with morphine dependence and naloxone-precipitated withdrawal. Brain Res. *905*, 254–258.

Punch, L.J., Self, D.W., Nestler, E.J., and Taylor, J.R. (1997). Opposite modulation of opiate withdrawal behaviors on microinfusion of a protein kinase A inhibitor versus activator into the locus coeruleus or periaqueductal gray. J. Neurosci. *17*, 8520–8527.

Quick, M.W. (2002). Substrates regulate γ-aminobutyric acid transporters in a syntaxin 1A-dependent manner. Proc. Natl. Acad. Sci. USA *99*, 5686–5691.

Risso, S., DeFelice, L.J., and Blakely, R.D. (1996). Sodium-dependent GABA-induced currents in GAT1-transfected HELA cells. J. Physiol. *490*, 691–702.

Schoffelmeer, A.N.M., Vanderscjirem, L.J.M.J., De Vries, T.J., Hogenboom, F., Wardeh, G., and Mulder, A.H. (2000). Synergistically interacting dopamine D1 and NMDA receptors mediate nonvesicular transporter-dependent GABA release from rat striatal medium spiny neurons. J. Neurosci. *20*, 3496–3503.

Sharma, S.K., Klee, W.A., and Nirenberg, M. (1975). Dual regulation of adenylate cyclase accounts for narcotic dependence and tolerance. Proc. Natl. Acad. Sci. USA *72*, 3092–3096.

Shen, K.Z., and North, R.A. (1992). Muscarine increases cation conductance and decreases potassium conductance in rat locus coeruleus neurones. J. Physiol. *455*, 471–485.

Stinus, L., LeMoal, M., and Koob, G.F. (1990). Nucleus accumbens and amygdala are possible substrates for the aversive effects of opiate withdrawal. Neuroscience *37*, 767–773.

Suzdak, P.D., Frederiksen, K., Andersen, K.E., Sorensen, P.O., Knutsen, L.J.S., and Nielsen, E.B. (1992). NNC-711, a novel potent and selective γ-aminobutyric acid uptake inhibitor: pharmacological characterization. Eur. J. Pharmacol. *224*, 189–198.

Svoboda, K.R., and Lupica, C.R. (1998). Opioid inhibition of hippocampal interneurons via modulation of potassium and hyperpolarization-activated cation (I_h) currents. J. Neurosci. *18*, 7084–7098.

Terwilliger, R.Z., Beitner-Johnson, D., Sevarino, K.A., Crain, S.M., and Nestler, E.J. (1991). A general role for adaptations in G-proteins and the cyclic AMP system in mediating the chronic actions of morphine and cocaine on neuronal function. Brain Res. *548*, 100–110.

Vaughan, C.W., Bagley, E.E., Drew, G., Hack, S., Pintar, J.E., Schuller, A.G.P., and Christie, M.J. (2003). Cellular actions of opioids on periaqueductal grey neurons from C57B16/J mice and mutant mice lacking MOR-1. Br. J. Pharmacol. *139*, 362–367.

Whitworth, T.L., and Quick, M.W. (2001). Substrate induced regulation of γ-aminobutyric acid transporter trafficking requires tyrosine phosphorylation. J. Biol. Chem. *276*, 42932–42937.

Williams, J.T., Christie, M.J., and Manzoni, O. (2001). Cellular and synaptic adaptations mediating opioid dependence. Physiol. Rev. *81*, 299–343.